UNAFLOW project: UNsteady Aerodynamics of FLOating Wind turbines

Bayati, I.; Belloli, M.; Bernini, L.; Boldrin, D.M.; Boorsma, K.; Caboni, M.; Cormier, M.; Mikkelsen, R.; Lutz, T.; Zasso, A.

Published in:
Journal of Physics: Conference Series

Link to article, DOI:
10.1088/1742-6596/1037/7/072037

Publication date:
2018

Document Version
Publisher's PDF, also known as Version of record

UNAFLOW project: UNsteady Aerodynamics of FLOating Wind turbines

IOP Conf. Series: Journal of Physics: Conf. Series **1037** (2018) 072037 doi:10.1088/1742-6596/1037/7/072037

UNAFLOW project: UNsteady Aerodynamics of FLOating Wind turbines

I.Bayati[1*], M. Belloli[1], L.Bernini[1], D.M.Boldrin[1], K.Boorsma[2], M.Caboni[2], M.Cormier[3], R.Mikkelsen[4], T. Lutz[3], A.Zasso[1]

1:Politecnico di Milano (PoliMI), Department of Mechanical Engineering, Milano, Italy
2:Energy research Centre of the Netherlands (ECN), LE Petten, The Netherlands
3:University of Stuttgart (USTUTT), Stuttgart, Germany
4:Technical University of Denmark (DTU), Department of Wind Energy, Lyngby, Denmark

E-mail: ilmasandrea.bayati@polimi.it

Abstract. UNAFLOW (UNsteady Aerodynamics for Floating Wind) is a joint EU-IRPWIND founded experiment on wind turbine rotor unsteady aerodynamics. It brings together four different academic contributors: Energy research Centre of the Netherlands (ECN), DTU Wind Energy, University of Stuttgart (USTUTT) and Politecnico di Milano (PoliMi) sharing knowledge both in numerical modelling and in experimental tests design, allowing direct numerical and experimental comparison.

The experimental tests carried out for UNAFLOW are of the same type of the ones carried out during the ongoing EU H2020 project LIFES50+ [1], regarding both the unsteady behaviour of the 2d blade section and the entire turbine rotor, although with improved setup and wider test matrix.

The project partners are already currently jointly collaborating in the AVATAR project [2], developing and validating numerical models of different accuracy level. The numerical models used in the UNALFOW project range from engineering tool (eg. BEM) to high fidelity CFD methods. Numerical simulations are used both in the design of experiment phase and in the results analysis allowing for an in depth understanding of the experimental findings through advanced modelling approach.

The UNAFLOW project, together with a new understanding of the unsteady behaviour of the turbine rotor aerodynamics, will provide also an open database to be shared among the scientific community for future analysis and new models validation.

1. Introduction

UNAFLOW project focus is the advanced aerodynamic modelling and novel experimental approaches about unsteady behaviour of Multi-Megawatt wind turbines rotors. The motivation of this new research effort lies within the increased interest in offshore floating wind energy systems.

Floating wind turbines allow to place the wind farm in deep water regions unlocking new energy source possibilities, but at the same time require an improved knowledge in the aerodynamic response of rotors subjected to the strong motion possible in high waves condition. For this reason a series of simplified but representative tests were designed, the aerodynamic of the rotor is studied in term of blade 2d section (sect.2), and entire rotor response (sect.3) The unsteadiness is considered as harmonic oscillations of the angle of attack on the blade section

and in the surge direction (i.e. translation displacement in the wind direction) for the whole turbine.

Experimental measurements were performed at the DTU red wind tunnel, described in sect.2.1, for the 2d aerodynamics and at PoliMi wind tunnel, described in sect.3.1, for the full rotor. Numerical model include 2d and 3d CFD models from USTUTT, described in sect.2.2-3.3, and engineering methods, specifically BEM and free vortex lifting line, from ECN, described in sect.3.2.

2. Unsteady 2d aerodynamics

2.1. Experimental facility description:DTU red wind tunnel

The DTU tunnel tunnel is an open loop tunnel with a cross section measuring $500x500mm^2$, a contractions ratio of 12.5 and capable of speeds up to U=65m/s. The tunnel is instrumented with a turntable for setting aerofoil AOA. A single component force gauge is embedded into the turn table measuring lift only. A Pitot tube at the inlet measuring the reference tunnel speed.

The wing model for testing the SD7032 is made from carbon fabric and CNC milled steel parts. It has 32 tabs at midspan, in line with the flow measured by a pressure modules from PSI Pressure Systems with 32 ports and range of $\pm 1psi$.

The flow quality was measured in terms of turbulence intensity (TI) using single component hotwire probe from Dantec Dynamics at the position of the 0.25 of the wing model chord. Velocities of 5.7, 8.6, 11.5 and 17.3m/s equivalent to chord Reynolds number of 50k,75k,100k,150k are measured.

The TI resulted equal to 0.04% at all tested Reynolds numbers, since the PoliMi wind tunnel that will be used for the full turbine tests, see Sect.3.1, it characterized by an higher turbulence level, the possibility to increase the DTU wind tunnel turbulence by adding three thin wires was considered. A wire of 0.15 mm diameter was placed in the flow about 4 chords upstream covering full span of the 2D wing. Turbulence index increased to 0.3% at 100k that was considered more representative of the PoliMi wind tunnel flow.

2.2. numerical model description:FLOWer 2d simulation

2D CFD simulations of the SD7032 airfoil have been performed with the FLOWer software, described fully in Sect.3.3, to deliver polars and study the boundary layer sensitivity to the wind tunnel turbulence intensity. The coordinates of the SD7032 airfoil have been obtained from the airfoiltools databank (www.airfoiltools.com) and the coordinates refined at the leading and trailing edges in the open-source, panel-based software Xfoil. The CFD CH-mesh, made of 119000 cells, has been built in Pointwise with fully resolved boundary layer according to the Reynolds number. The boundary layer contains 60 cells and there are 317 grid points around the airfoil. The simulations have been performed in fully turbulent boundary layer conditions. To close the equation system the Menter SST turbulence model is used.

2.3. 2d polars

Both steady and unsteady measurements were performed.

The steady measurements are carried out for Re=50k, 60k, 75k, 100k, 150k and 200k in smooth flow (clean) and with added inlet wire (wire) .

Figure 1(a) reports the 50k Reynolds comparison with FLOWer simulations, numerically is not possible to catch the non-linearity in the lift and drag curve close to 5 deg. This behaviour is probably due to a laminar separation on the airfoil suction side. In the wire polars the non-linear part is smeared out increasing the matching with numerical results. Increasing the Reynolds number to 100k in figure 1(b) the non-linearity in the experimental results is not present and thus the matching with numerical simulation is improved, the lift and drag values are predicted by numerical simulation with limited deviation only near the stall region.

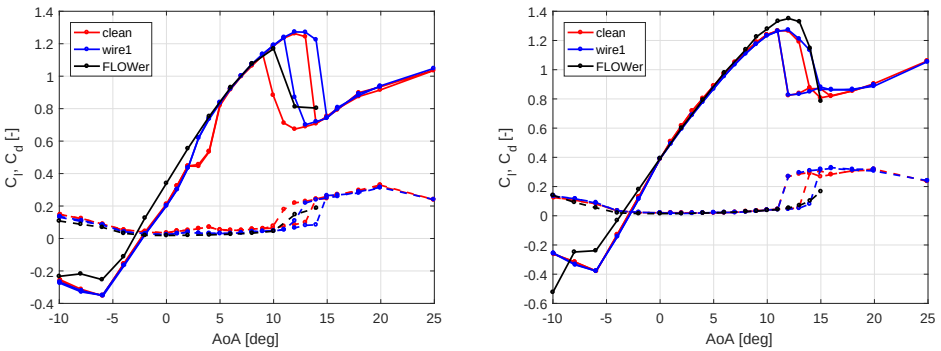

(a) Re=50k (b) Re=100k

Figure 1. SD7032 steady polar DTU measurements vs FLOWer 2d simulations

Unsteady pitching of the foil is carried out at Re=50k, 100k and 150k for mean AOA = 0,3,6,9,10,12,15 deg. Pitching amplitudes of 0.5,1,2 and 5 deg and frequencies 0.25, 0.5, 1, 2 and 3Hz. An example of the results is showed in figure 2 and figure 3, referring to the turbulence (wire) SD7032 response at Reynolds number 50k and 100k with angle of attack oscillation of 5 deg. An hysteretic cycle is always present when the airfoil is pitched near the stall angle, this hysteretic effect is increasing in strength at higher motion frequency and more important is appearing also in the linear region.

This finding goes in the direction of including dynamic airfoil response in turbine rotor unsteady conditions analysis. In the UNAFLOW project there was not a specific effort to reproduce numerically the unsteady airfoil behaviour, however, a wide dataset of unsteady polars are provided as project output. This data could be potentially used both to validate dynamic stall model or unsteady CFD computation aiming to catch lift and drag oscillation due to angle of attack dynamic variation.

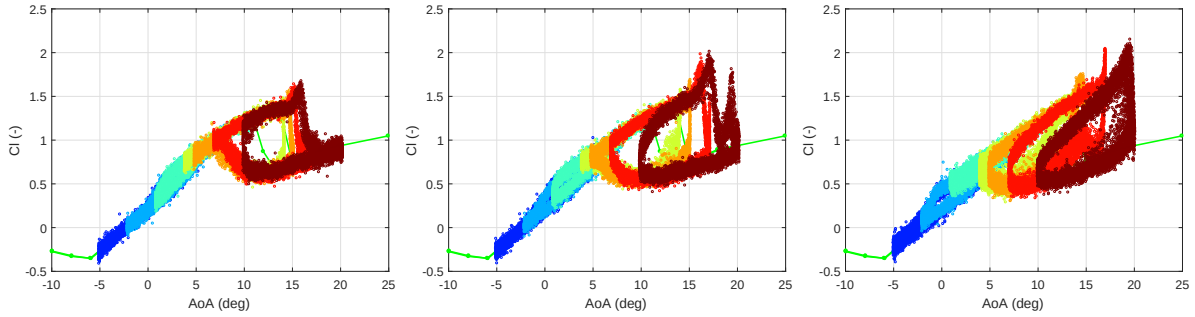

(a) $\Delta AOA = 5°; f = 0.5Hz$ (b) $\Delta AOA = 5°; f = 1Hz$ (c) $\Delta AOA = 5°; f = 2Hz$

Figure 2. Unsteady polar wire SD7032 Re=50k

3. Unsteady full turbine aerodynamics

3.1. Experimental facility description:POLIMI wind tunnel and turbine model

The PoliMi wind tunnel or GVPM [3] (Galleria del Vento of Politecnico di Milano) is a special closed-circuit wind tunnel, arranged in a vertical layout with two test rooms located on the opposites sides of the loop. The UNALFOW wind tunnel tests are going to be performed in the

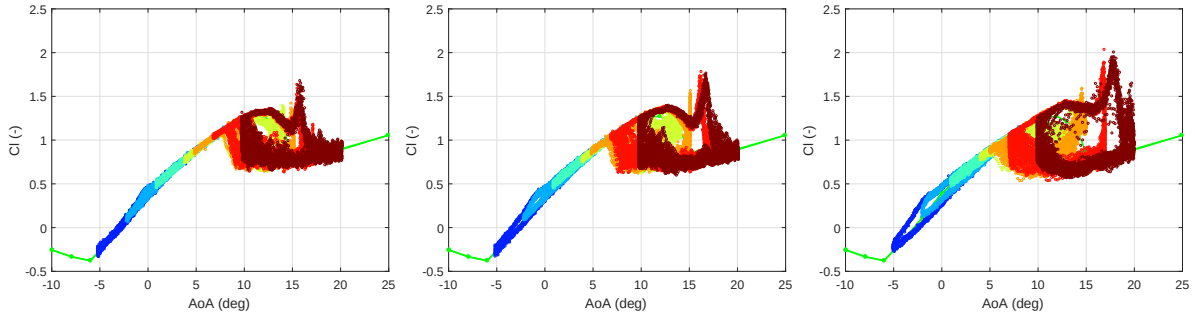

(a) $\Delta AOA = 5°; f = 0.5Hz$ (b) $\Delta AOA = 5°; f = 1Hz$ (c) $\Delta AOA = 5°; f = 2Hz$

Figure 3. Unsteady polar wire1 SD7032 Re=100k

upper leg of the wind tunnel loop that hosts the large Boundary Layer Test Section, which is 13.84m wide x 3.84m high. The maximum wind speed is 16m/s, a series on spires and roughness elements can be placed at the inlet section to simulate different turbulent ABL conditions. For the UNAFLOW project the wind tunnel will be used in empty inlet section configuration aiming to a constants wind profile. However, it is impossible to have a perfectly uniform wind flow because of tunnel walls effect and turbulence generated by the fans and nets of the tunnel circuits.

Figure 4 shows the measured vertical wind speed profile, normalized by the wind speed at hub height, and turbulence index for the wind tunnel in the UNAFLOW configuration. The wind speed can be considered constant from 0.5m above the ground and up to 0.3 m from the ceiling with a turbulence index close to 2

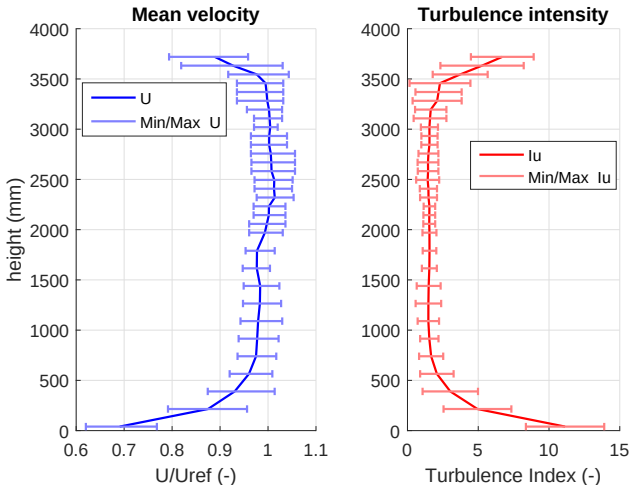

Figure 4. Polimi Wind tunnel flow characteristics with uncertainty range

The turbine model was designed and built to scale the salient aerodynamic and structural characteristic of the DTU10MW RWT [4]. Great care was taken in correctly match the scaled thrust force which can be considered the more important aerodynamic contribution in the floating system motion [5]. The turbine model is mounted on a test rig moved by two hydraulic actuators. The surge actuator is grounded on the wind tunnel floor and the pitch actuator mounted on the slider providing the pitch motion by means of a slider-crank mechanism. The

schematics of the test rig is showed in Figure 5, the pitch actuator impose a constant angle to the turbine to cancel the turbine tilt angle, i.e. the rotor plane is perfectly perpendicular to the ground. This choice was made to make the rotor aerodynamics simpler avoiding periodic effect due to the turbine tilt. All the steady and surge motion tests were done with this constant pitch angle.

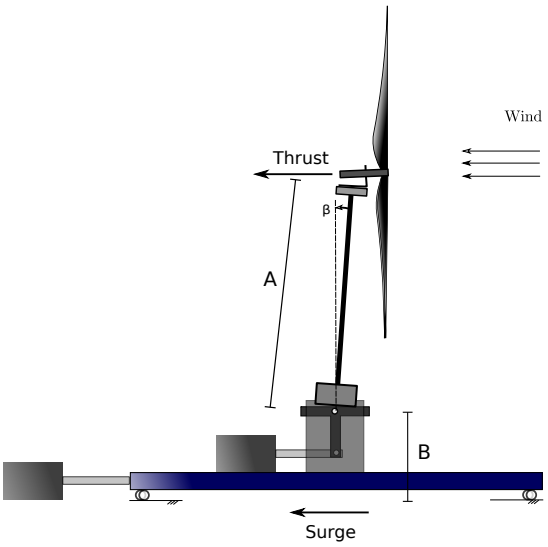

Figure 5. Turbine test rig main dimensions and reference system, A=1605 mm; B=450 mm ; $\beta = 5°$

The force measurements on the model are carried out using a six-component balance, ATI Mini45 SI-145-5, fixed at the tower top measuring the constraint force between the rotor and the tower. The test rig displacement is measured with a laser sensor, MEL M5L/200, able to guarantee high accuracy and sampling frequency. Figure 5 shows the measured trust and surge displacement positive direction

Beside the force measurement also the wake analysis using Particle Image Velocimetry (PIV) was performed. The PIV system can be used for measuring the two velocity components of the turbine wake in the vertical plane behind the wind turbine. A windows of 800 mm by 750 mm is acquired 600 mm behind the rotor plane capturing the turbine near wake structure. More details on the PIV system and results can be found in [6].

3.2. numerical model description: ECN Aero-Module simulation

Aero-Module is an ECN software featuring current state-of-the-art wind turbine aerodynamic models [7]. The two aerodynamic methods included in Aero-Module are respectively a method based on the classical blade element momentum (BEM) theory, and a method based on the free vortex wake model coupled to the lifting line model, named Aerodynamic Wind turbine Simulation Module (AWSM) [8]. In AWSM the blade geometry is modeled by means of a number of sections carrying a vortex ring, extending from the quarter chord position to the trailing edge. The free wake vortices' convection velocity is determined by the local wind velocity and by the induced velocity of all the surrounding blade bound and free wake vortices. The loads along the blade are estimated from user-prescribed two-dimensional (2D) lift and drag coefficients as a function of the angle of attack, assuming local 2D flow.

The unsteady simulations of the turbine undergoing surge motions were performed using both BEM and AWSM models, by specifying, as input, the rotor kinematics and blade sectional polars. The polars used for these simulations are those determined experimentally by DTU under clean and low turbulence conditions (i.e., without wire). All calculations were performed with a time step of 0.00691 s which corresponds to a step of 10 in rotor azimuth. Both BEM and AWSM calculations were performed using a correction model for rotational effect developed by Snel [9] In addition to this model, BEM calculations featured the Snels first order dynamic stall model [10] and dynamic inflow model [11].

3.3. numerical model description: FLOWer CFD simulation

The CFD simulations have been performed with a numerical chain for wind turbine simulations established at the Institute of Aerodynamics and Gas Dynamics (IAG, University of Stuttgart) [12][13]. Core of the simulation chain is the flow solver FLOWer. The code solves the finite three dimensional, compressible (Unsteady) Reynolds-Averaged Navier-Stokes equations ((U)RANS). To close the Navier Stokes equations, turbulence can be modeled either by algebraic models or by transport equation models, like the Menter Shear Stress Transport model[14].

Simulations of a one third model of the rotor (which means only one blade, a third of the spinner and a third of an axisymmetrical cylinder shaped background) have been performed. The wind tunnel environment, comprising the effects of the blockage ratio, of the tower and nacelle and the inflow velocity profile is not taken into account, future simulation are planned considering the full rotor and the wind tunnel effects. The total set up contains 13 Millions cells. The simulations are performed with uniform inflow conditions at the rated operational conditions of the wind turbine, u=4 m/s and 241 rpm. The Menter Shear Stress Transport turbulence model is used in fully turbulent conditions.

3.4. unsteady thrust results

The turbine response was measured at wind tunnel speed of 4m/s, the turbine was operated at its rated condition fixing the TSR was fixed at 7.5 equal a rotor model velocity of 241 RPM and 0° collective blade pitch angle. At this working condition a large number of frequency, between 0.125 Hz and 2 Hz, and amplitude, between 0.125 m to 0.008 m, of surge harmonic motion has been tested in the wind tunnel.

A subset of two conditions are selected for an initial comparison with numerical results. One at medium motion frequency (1Hz at 35 mm amplitude) and one at high motion frequency (2Hz at 8 mm amplitude). Figures 6(a)-(b) show the comparison of the thrust force measured during the wind tunnel tests compared with ECN calculation using BEM and AWSM and the FLOWer CFD results. The average was removed from all the results; therefore, the graphics are showing the thrust oscillation due to the surge motion of the turbine. Wind tunnel signal is affected by higher frequency oscillation due mainly to mechanical spurious effect (rotor mass disbalance, vibrations of the test rig platform,), turbulence in wind tunnel flow and instruments noise.

To make the comparison easier a mono-harmonic filter is applied to the force signals. The filtered signals are indicated as 'EXP 1 arm' for both the considered cases. The numerical-experimental matching of the thrust oscillation is good amplitude in particular for BEM calculation. There is however a phase shift between the signals.

Looking at only the response component at the considered surge frequency some more quantitative comparisons are possible A broader case selection is considered (note that FLOWer results are not available for this broader selection)

Figure 7(a) shows the comparison of experimental and numerical findings in terms of amplitude of thrust oscillation divided by surge motion amplitude and phase shift between thrust and surge position. The black crosses refer to the wind tunnel results, the dots are the numerical computation in red for BEM and in blue for AWSM, the green square are the

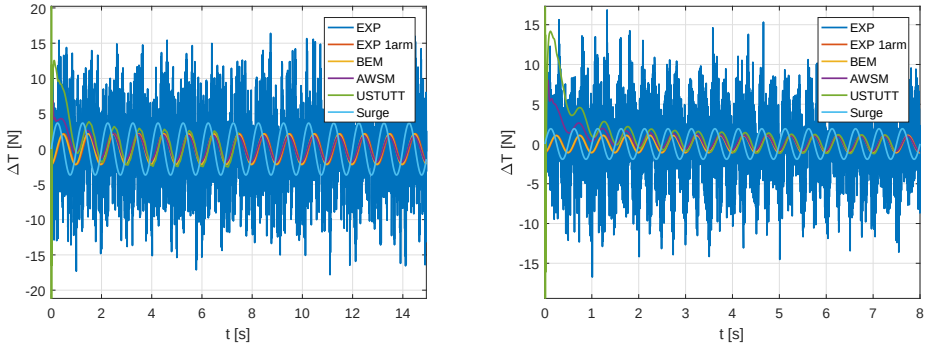

(a) f=1Hz A=35 mm not filtered (b) f=2Hz A=8 mm not filtered

Figure 6. Thrust oscillation experimental vs numerical comparison (Surge motion not in scale)

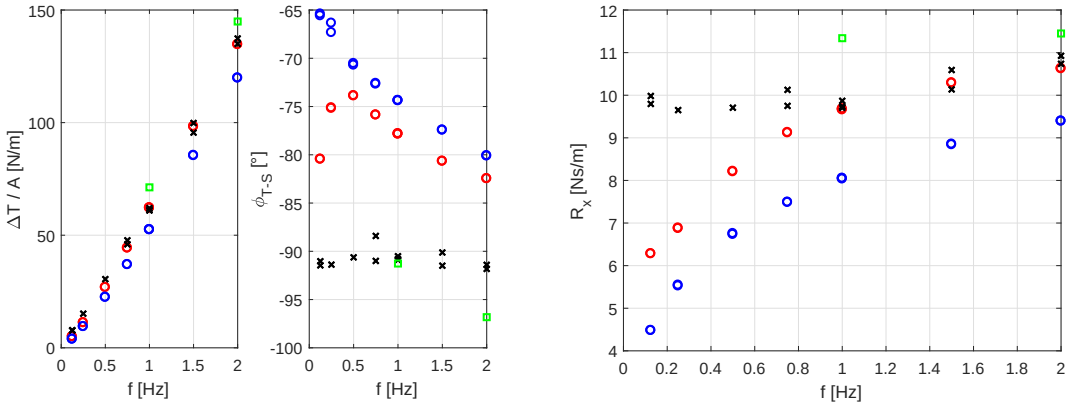

(a) Amplitude and phase of thrust oscillation (b) Equivalent damping value of thrust

Figure 7. Thrust force unsteady analysis

FLOWer simulations. From the two graph it is possible to observe that also for this bigger set of cases there is a good agreement of thrust amplitude oscillation between BEM and wind tunnel and slightly lower matching for AVSM computations. The wind tunnel results present a phase almost constantly fixed at -90 while numerical results show a variation function of the surge frequency (FLOWer CFD results are not numerous enough for any trend consideration). To have a more physical understanding of the results is useful to look at unsteady thrust response as an equivalent damping effect (a perfect dumper will result in a perfect -90 phase shift). Figure 7(b) is the equivalent damping value of the thrust calculated as:

$$R_x = -T \sin(\phi_{T-S})/(A \cdot 2\pi f)$$

In terms of equivalent damping the wind tunnel and FLOWer results show a close to constant value in agreement with the constant phase value of thrust. ECN models show a strong variation of damping value in function of motion frequency, due to the phase variation observed in the numerical results.

This behaviour is motivated by the dynamic inflow and stall models used by ECN aerodynamic code that are responsible for the time lag between the motion of the turbine and the thrust response of the rotor or equivalently the phase shift in the frequency domain.

The reason why this time-lag/phase-shift is not present in the experimental results is still an open question, the comparisons with other numerical codes could be beneficial in the understanding of the physical motivation of this discrepancy in the results between numerical methods and experiment.

3.5. Unsteady wake analysis

Beside the rotor loads, the wake dynamics are of particular interest when designing wind turbines, since they have an influence on the rotor performance and, when installed in a wind farm, on the downstream turbines.

Figure 8(a) shows the wake vorticity from different PIV acquisitions taken at four surge positions for the f=1 Hz and 35 mm amplitude surge motion case. In clockwise order, and referring to the scheme of figure 5, the positions of the PIV are the point A-B-C-D as reported in talbe 1.

Table 1. PIV acquisition points description (BDC:bottom dead center TDC:top dead center)

	Surge Position	**Surge Velocity**
A	min (BDC)	zero
B	zero	max (against wind)
C	max (TDC)	zero
D	zero	min (along wind)

Figure 8(b) shows the same vorticity slice from FLOWer simulations at the same surge position of the PIV wind tunnel acquisitions.

In both experiments and numerical results the tip vortex trace is clearly visible however some important differences are present:

- Numerical tip vortex is more smeared probably due to high numerical viscosity
- The tip vortex position is different in PIV and numerical results and this is due to the fact that images of PIV and flower have a constant rotor position (since the rotor rotational frequency is 4 times the surge one) but there is no matching between the two.

Both FLOWer and PIV agree on the effect of motion on the tip vortex, looking at both it is visible a relative displacement of the vortex core cycling trough the different acquired surge position. In standard no surge motion condition one should expect to find the vortex core at the same position in the four images for being the rotor position fixed. However the vortex core is moving in the surge direction due to the turbine motion, this prove that the turbine near wake is affected by the turbine motion. A more precise analysis of the turbine motion effects on the rotor wake can be found in [6]

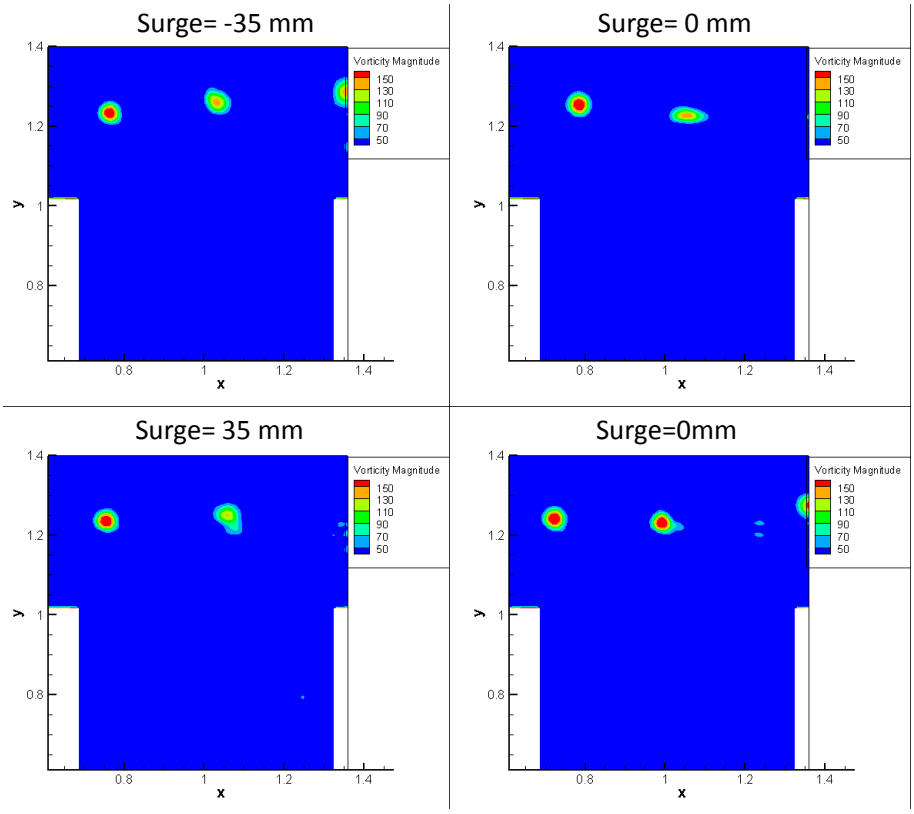

(a) Wind Tunnel PIV

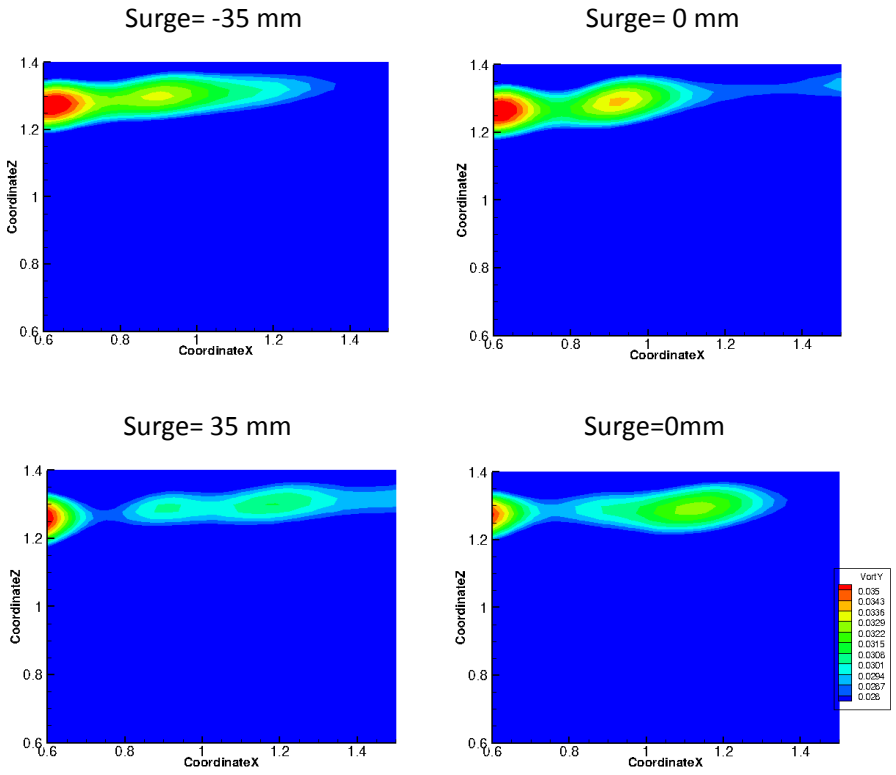

(b) FLOWer

Figure 8. vorticity slice of the wake PIV vs numerical simulation for f=1Hz A=35 mm in clockwise order point A-B-C-D of table 1, coordinates in meter

4. Conclusion

The project was focused in the analysis of simple conditions, the pitching oscillation effect on the blade airfoil aerodynamics and the surge motion on the full rotor response, on the other hand, a great number of different combinations of frequency and amplitude was taken into consideration.

The most important outcome of the UNAFLOW project is the wide database of unsteady turbine aerodynamics in imposed motion conditions. Both for the blade sectional airfoil and the full turbine rotor.

This will be useful for numerical code validation purposes as already introduced in this work and more deeply described in [15], and will hopefully help in understanding the underlaying physics of unsteady turbine aerodynamics possibly resulting in the synthesis of new formulation able to correctly predict the turbine response to high structural motion.

The results presented in this article are just a selection of all the wind tunnel tested conditions, the data are freely available, as requested for IRPWIND founded project. Data are stored in a FTP sever, more information on the database access can be found at www.unaflow.mecc.polimi.it.

Aknowledgments

This research has been funded by EU-EERA (European Energy Research Alliance)/IRPWIND Joint Experiment 2017.

References

[1] I. Bayati, M. Belloli, L. Bernini, and A. Zasso, Wind tunnel validation of AeroDyn within LIFES50+ project: Imposed Surge and Pitch tests, J. Phys. Conf. Ser., vol. 753, no. 9, 2016.
[2] http://www.eera-avatar.eu/ or J.G. Schepers O. Ceyhan, K. Boorsma, A. Gonzalez, X Munduate, O Pires, N.Srensen, C. Ferreira, G Sieros, J. Madsen, S. Voutsinas, T. Lutz, G. Barakos, S. Colonia, H. Heielmann, F. Meng and A. Croce Latest results from the EU project AVATAR: Aerodynamic modelling of 10 MW wind turbines, The Science of Making Torque conference, October 2016
[3] Politecnico di Milano, Wind Tunnel. [Online]. Available: http://www.windtunnel.polimi.it/.
[4] C. Bak et Al, "The DTU 10-MW Reference Wind Turbine",Technical University of Denmark, DTU Wind Energy, Denmark, 2013.
[5] Bayati, I., Belloli, M., Bernini, L., Zasso, A. Aerodynamic design methodology for wind tunnel tests of wind turbine rotors (2017) Journal of Wind Engineering and Industrial Aerodynamics, 167, pp. 217-227.
[6] I.Bayati, L.Bernini, A.Zanotti, M.Belloli, A.Zasso. Experimental investigation of the unsteady aerodynamics of FOWT through PIV and hot-wire wake measurements, The Science of Making Torque conference, June 2018 (forthcoming)
[7] G. F. Boorsma K e J. Holierhoek, Enhanced approach for simulation of rotor aerodynamic loads, Amsterdam, 2011.
[8] A. v. Garrel., Development of a wind turbine aerodynamics simulation module., ECN, 2003.
[9] B. Montgomerie, A. Brand, J. Bosschers e R. V. Rooij, Three-dimensional effects in stall, 1996.
[10] H. Snel, Heuristic modelling of dynamic stall characteristics, 1997.
[11] H. Snel e J. G. Schepers, Joule1: Joint investigation of dynamic inflow effects and implementation of an engineering model, 1994
[12] P. Kranzinger, Automatisierte Generierung von Rechnegittern zur Tragflgel- und Rotorblattoptimierung, Master thesis, 2011.
[13] N. Kroll e J. Fassbender, MEGAFLOW Numerical Flow Simulation for Aircraft Design, Springer Verlag Berlin/Heidelberg/New York; ISBN 3-540-24383-6;, 2002.
[14] F. R. Menter, Two-equation eddy-viscosity turbulence models for engineering applications, AIAA journal, vol. 32(8), pp. 1598-1605, 1994.
[15] M.Cormier, M.Caboni, T.Lutz, K.Boorsma, E.Kraemer Numerical analysis of unsteady aerodynamics of floating offshore wind turbines. The Science of Making Torque conference, June 2018 (forthcoming)